

# Monocular Open Vocabulary Occupancy Prediction for Indoor Scenes

Changqing Zhou<sup>1</sup> Yueru Luo<sup>2</sup> Han Zhang<sup>1</sup> Zeyu Jiang<sup>1</sup> Changhao Chen<sup>1</sup>✉

<sup>1</sup> The Hong Kong University of Science and Technology (Guangzhou)

<sup>2</sup> The Chinese University of Hong Kong, Shenzhen

czhou149@connect.hkust-gz.edu.cn changhaochen@hkust-gz.edu.cn

## Abstract

Open-vocabulary 3D occupancy is vital for embodied agents, which need to understand complex indoor environments where semantic categories are abundant and evolve beyond fixed taxonomies. While recent work has explored open-vocabulary occupancy in outdoor driving scenarios, such methods transfer poorly indoors, where geometry is denser, layouts are more intricate, and semantics are far more fine-grained. To address these challenges, we adopt a geometry-only supervision paradigm that uses only binary occupancy labels (occupied vs. free). Our framework builds upon 3D Language-Embedded Gaussians, which serve as a unified intermediate representation coupling fine-grained 3D geometry with a language-aligned semantic embedding. On the geometry side, we find that existing Gaussian-to-Occupancy operators fail to converge under such weak supervision, and we introduce an opacity-aware, Poisson-based approach that stabilizes volumetric aggregation. On the semantic side, direct alignment between rendered features and open-vocabulary segmentation features suffers from feature mixing; we therefore propose a Progressive Temperature Decay schedule that gradually sharpens opacities during splatting, strengthening Gaussian-language alignment. On Occ-ScanNet, our framework achieves 59.50 IoU and 21.05 mIoU in the open-vocabulary setting, surpassing all existing occupancy methods in IoU and outperforming prior open-vocabulary approaches by a large margin in mIoU. Code will be released at <https://github.com/JuIvyy/LegoOcc>.

## 1. Introduction

Comprehensive 3D geometric and semantic understanding of surrounding environments is fundamental for embodied agents across diverse applications such as service robots, drones, and AR/VR systems. Within this context, *semantic occupancy* has emerged as a powerful and compact for-

✉Corresponding author.

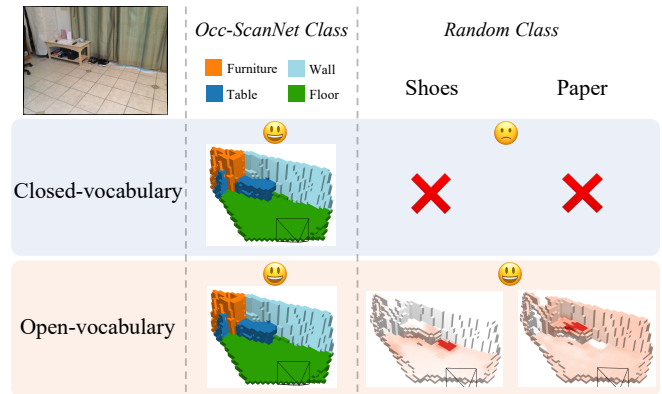


Figure 1. **Closed- vs. open-vocabulary occupancy.** Prior methods [47, 50] trained under a *closed vocabulary* can label only the categories predefined at training time, which restricts real-world deployment. Our *open-vocabulary* approach aligns language with 3D occupancy and supports text queries for arbitrary categories. *Right column (Random Class)*: text-conditioned per-voxel scores are visualized as heatmaps; darker red indicates higher likelihood for the queried category.

mulation that unifies dense geometry and semantics within a volumetric grid, enabling high-level spatial reasoning and downstream embodied decision-making [22, 23, 44]. Vision-centric occupancy prediction is particularly attractive due to the ubiquity, low cost, and rich appearance cues of cameras. Recent studies and benchmarks show that vision-only pipelines can infer competitive 3D occupancy from both *monocular* inputs [20, 39, 42, 47, 50, 51, 56] and *multi-view* inputs [7, 11, 13, 45], employing architectures ranging from transformer-based to Gaussian-splatting-based designs.

In general, occupancy prediction involves two key components: *geometry learning*, which determines whether a voxel is occupied, and *semantic learning*, which assigns a category to each occupied voxel. However, real-world deployments often encounter highly long-tailed category distributions [55] and inherently open-ended semantic spaces [15]. Consequently, restricting predictions to a fixed, closed vocabulary limits practical utility and motivates the

development of open-vocabulary occupancy prediction. As shown in Fig. 1, conventional closed-vocabulary models can only recognize training-time categories, whereas open-vocabulary formulations lift this restriction and significantly broaden real-world applicability.

This direction has progressed rapidly in outdoor driving scenarios, where recent methods integrate vision–language models (VLMs) and text prompts to associate camera-based 3D occupancy with free-form semantics [5, 19, 36, 53, 58]. By contrast, indoor occupancy prediction remains relatively underexplored and is typically trained or evaluated under small, closed taxonomies; for instance, Occ-ScanNet [50] defines only 11 semantic classes, which underrepresents the rich and diverse semantics of indoor environments. Indoor scenes further differ fundamentally from outdoor ones in *two critical aspects*: **1)** they exhibit much denser and more complex geometry, and **2)** they contain far more fine-grained, long-tailed semantic categories. As a result, directly applying outdoor open-vocabulary occupancy pipelines to indoor settings yields limited performance [47], as also evidenced in our experiments (see Tab. 1 and discussion in Sec. 4.3). Early attempts such as OVO [38] take an initial step by distilling 2D open-vocabulary segmentation into 3D voxels on smaller-scale datasets, but still rely on a fixed set of base categories during training. These limitations highlight both the practical importance and the open challenge of indoor open-vocabulary occupancy: embodied agents must reason about arbitrary objects and spatial layouts beyond a fixed label set before taking action, yet existing indoor methods fall short of this requirement.

To address this gap, we adopt a geometry-only supervision protocol: training uses only binary voxel occupancy labels and no semantic voxel annotations, and we tackle the resulting challenges on both the geometric and semantic fronts. This setting is practically motivated, as geometry can be harvested at scale with modest effort—for example, Occ-ScanNet constructs its occupancy ground truth via SC-Fusion [46], which incrementally fuses occupancy probabilities from depth-based reconstruction [40] and completion methods [3, 43]. In contrast, semantic labels remain expensive to curate due to the high diversity and long-tailed distribution of indoor categories.

To enable open-vocabulary occupancy prediction under geometry-only supervision, we employ 3D Language-Embedded Gaussians (LE-Gaussians) [33, 59] as the spatial intermediate representation. Each LE-Gaussian couples (1) native geometric parameters—position, rotation, scale, and opacity—that encode local occupancy evidence, with (2) a learnable semantic embedding that anchors language-aligned [30] semantics at a specific 3D location. **On the geometry side**, indoor environments contain dense structures and severe occlusions, demanding fine-grained volumetric modeling. While Gaussian primitives offer an ex-

pressive and computationally efficient representation, existing Gaussian-to-Occupancy (G2O) mappings become unstable when trained solely with binary occupancy labels due to insufficient opacity modeling (Sec. 3.3). To address this, we introduce an opacity-aware, *Poisson-based Gaussian-to-Occupancy* formulation. Our model treats each Gaussian’s effective opacity as a nonnegative event intensity and interprets voxel occupancy as the first-arrival event of a Poisson process, enabling stable and principled volumetric aggregation. **On the semantic side**, indoor categories are highly fine-grained and long-tailed, causing naïve alignment between rendered Gaussian features and 2D open-vocabulary segmentations to suffer from feature mixing when multiple categories overlap in image space (Sec. 3.4). Concretely, we render LE-Gaussian features into images via Gaussian splatting [17] and align them with features extracted by a training-free open-vocabulary segmenter (e.g., Trident [35]). To mitigate feature dilution caused by weighted feature aggregation, we introduce a *Progressive Temperature Decay* schedule that gradually sharpens effective opacities during splatting. This suppresses cross-category blending and yields more discriminative, language-aligned 3D features for indoor open-vocabulary occupancy prediction.

In summary, our contributions are threefold:

- We introduce **LEGOOcc**, which leverages Language-embedded Gaussians as a fine-grained 3D spatial intermediate representation for monocular **Open-vocabulary Occupancy** prediction in large-scale indoor environments, enabling embodied agents to reason about arbitrary objects beyond closed taxonomies.
- We propose an opacity-aware, Poisson-based Gaussian-to-Occupancy operator that operates reliably under geometry-only (binary) occupancy supervision. In addition, we develop a Progressive Temperature Decay schedule that sharpens Gaussian opacities during splatting, thereby enhancing Gaussian–language feature alignment.
- We conduct extensive experiments on Occ-ScanNet, where our framework achieves 59.50 IoU and 21.05 mIoU in the open-vocabulary setting, surpassing the previous SoTA by 3.02 IoU and outperforming prior open-vocabulary methods by 11.80 mIoU (more than 2× the best previous result); ablation studies further validate the effectiveness of each proposed component.

## 2. Related works

### 2.1. Occupancy Prediction

Camera-only occupancy has been extensively studied in outdoor autonomous driving, often using grid- or transformer-based pipelines [11, 13, 34], whereas indoor settings remain comparatively underexplored. MonoScene first cast semantic scene completion as an occupancy prediction task [6, 37, 49], and subsequent works on in-

door datasets such as Occ-ScanNet [50] improved accuracy and scalability. Notable methods include ISO [50] with depth-guided feature lifting, EmbodiedOcc [47] with Gaussian-based volumetric prediction, and RoboOcc [57] with opacity-guided encoders. Methodologically, indoor approaches span dense volumetric lifting of 2D features along rays into voxel grids followed by decoding with 3D CNNs or volumetric heads [6, 21, 28, 49, 50]. More recent works employ transformer-augmented volumetrics and sparse Gaussian/point primitives that iteratively refine geometry–semantics coupling for efficiency and fidelity [13, 42, 47, 57]. However, indoor environments differ markedly from structured road scenes in layout complexity, scale/viewpoint variation, and long-tailed distribution of fine-grained categories. Consequently, designs tailored for driving scenes often transfer suboptimally indoors, motivating a re-examination of feature lifting, spatial representation, and supervision paradigms [47, 50, 57].

## 2.2. Open Vocabulary Occupancy Prediction

Open-vocabulary occupancy has recently gained traction in autonomous driving as a way to mitigate the cost and difficulty of annotating 3D occupancy. These methods typically adopt self-/weakly supervised settings to learn voxel-level geometry and semantics without full 3D labels. For semantic learning, most approaches first derive open-vocabulary cues from VLMs and obtain pseudo 2D masks with open-set segmentors [24, 31]. These signals are then either lifted to 3D by projecting pixels onto point clouds or associating pixels/points with voxels [19, 53, 54], or mapped to voxels via differentiable voxel projection [41, 58], or used to supervise a rendered 3D semantic field directly in the image plane via volume rendering [5]. Feature alignment is commonly achieved through cosine similarity between voxel features and text/image embeddings [24, 31]. For geometry learning, two families dominate: LiDAR-derived pseudo labels aggregated into voxels for supervision [9, 19, 41, 58], and self-supervised multi-view rendering to learn occupancy by enforcing photometric/feature consistency across frames without 3D ground truth [12, 54].

In indoor scenarios, research remains limited. OVO [38] makes an early attempt on a small-scale dataset by distilling open-vocabulary semantics into a 3D occupancy network via pixel-wise alignment between projected voxel features and 2D open-vocabulary segmentation. OpenOcc [14] further leverages neural radiance fields to unifying the 3D scene reconstruction and understanding from RGB-D inputs, while OG [8] integrates grounded-SAM [31] with affinity fields to distinguish grounded instances. Despite these efforts, open-vocabulary occupancy for large-scale indoor scenes remains largely underexplored.

## 3. Method

### 3.1. Problem Setting

Given an input image  $\mathbf{I} \in \mathbb{R}^{H \times W \times 3}$ , the goal of occupancy estimation is to predict a semantic occupancy field  $\mathbf{O} \in \mathbb{R}^{X \times Y \times Z \times C}$ , where  $(X, Y, Z)$  specify the resolution of the local 3D volume and  $C$  is the number of semantic categories. We decompose the problem into two complementary components: (i) *geometry learning*, which determines whether each voxel is occupied, and (ii) *semantic learning*, which assigns a category to occupied voxels.

To enable open-vocabulary occupancy, we employ *Language-Embedded Gaussians* (LE-Gaussians) as a unified 3D intermediate representation coupling geometry and language-aligned semantics. Each LE-Gaussian is parameterized as:

$$\mathcal{G}_i = (\boldsymbol{\mu}_i, \boldsymbol{\Sigma}_i, \alpha_i, \mathbf{f}_i), \quad (1)$$

where  $\boldsymbol{\mu}_i \in \mathbb{R}^3$  and  $\boldsymbol{\Sigma}_i \in \mathbb{R}^{3 \times 3}$  are the Gaussian center and covariance,  $\alpha_i \in [0, 1]$  denotes opacity, and  $\mathbf{f}_i \in \mathbb{R}^d$  is a language-aligned embedding with  $d$  channels. LE-Gaussians thus explicitly bind *geometry* (via  $\boldsymbol{\mu}_i, \boldsymbol{\Sigma}_i, \alpha_i$ ) and *open-vocabulary semantics* (via  $\mathbf{f}_i$ ) within a single set of primitives, supporting both occupancy prediction and semantic reasoning.

### 3.2. LegoOcc Framework Overview

As illustrated in Fig. 2, given an input image  $\mathbf{I}$ , a feed-forward Gaussian predictor outputs a set of LE-Gaussians  $\mathbf{G} = \{\mathcal{G}_i\}_{i=1}^N$ . The same set  $\mathbf{G}$  is then reused for two purposes: 1) *occupancy prediction* (Sec. 3.3), where our Poisson-based Gaussian-to-Occupancy (G2O) operator infers 3D occupancy from geometric parameters  $(\boldsymbol{\mu}_i, \boldsymbol{\Sigma}_i, \alpha_i)$ ; and 2) *language-aligned semantic prediction*, where per-Gaussian embeddings  $\mathbf{f}_i$  are used to infer the semantic label of each occupied voxel. Supervision is imposed by rendering these embeddings to the image plane and aligning the rendered features with those from open-vocabulary segmentation models; the alignment is further improved by our progressive temperature decay (Sec. 3.4). Training jointly minimizes a supervised binary-occupancy loss with ground-truth and a rendered-feature alignment loss that requires no 2D human annotations; see Sec. 3.5 for details.

### 3.3. Poisson-based Gaussian-to-Occupancy

3D Gaussians offer an efficient and expressive representation to capture fine-grained indoor geometry and have been widely adopted for scene reconstruction. In this section, we first revisit Gaussian splatting, analyze why existing G2O formulations become problematic under binary-only occupancy supervision, and then introduce our Poisson-based G2O reformulation that addresses the issue.

**Gaussian Splatting.** We follow the front-to-back  $\alpha$ -blending strategy of Gaussian Splatting [17] to render im-

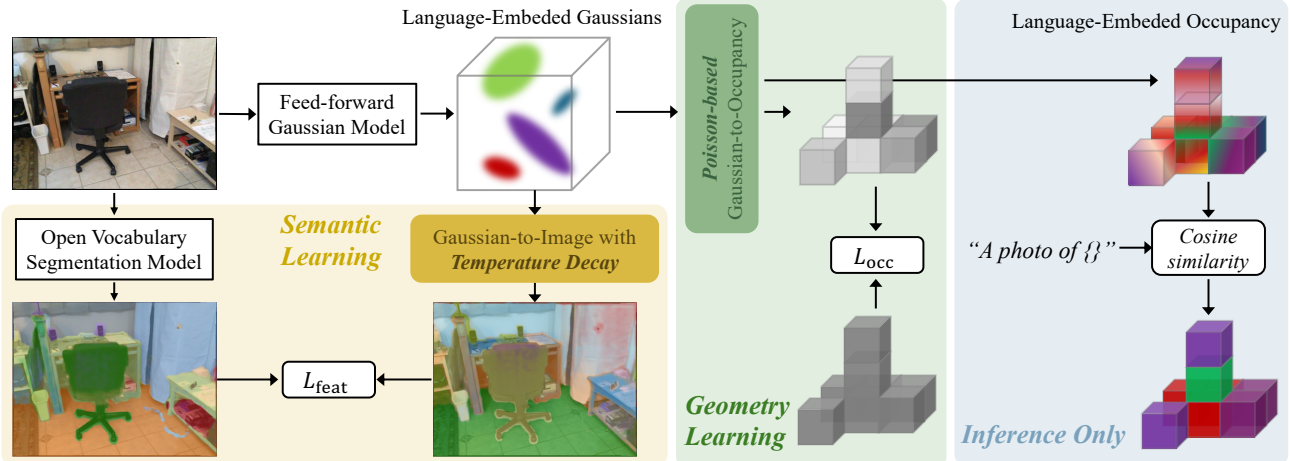


Figure 2. **LegoOcc Framework Overview.** From a monocular image, a feed-forward Gaussian model produces *Language-Embedded Gaussians*. Training proceeds along two couched paths: *Semantic learning*, we differentially render Gaussian features to the image with *Progressive Temperature Decay* and align them to a training-free open-vocabulary segmenter via a cosine objective  $L_{\text{feat}}$ ; *Geometry learning*, we convert Gaussians to occupancy using an opacity-aware Poisson-based Gaussian-to-Occupancy operator and supervise binary occupancy with  $L_{\text{occ}}$ . At inference, the *Language-Embedded Occupancy* supports text-driven queries by computing cosine similarity between voxel embeddings and prompt embeddings, yielding open-vocabulary semantic occupancy without dense voxel-level semantic labels during training.

age features from LE-Gaussians. For the  $i$ -th Gaussian  $\mathcal{G}_i$  with color  $\mathbf{c}_i$ , opacity  $\alpha_i \in [0, 1]$ , and screen-space mean/covariance  $(\boldsymbol{\mu}'_i, \boldsymbol{\Sigma}'_i)$ , its 2D kernel at image location  $\mathbf{x}'$  is

$$p_i(\mathbf{x}') = \exp\left(-\frac{1}{2}(\mathbf{x}' - \boldsymbol{\mu}'_i)^\top \boldsymbol{\Sigma}'_i^{-1}(\mathbf{x}' - \boldsymbol{\mu}'_i)\right), \quad (2)$$

where primes denote screen-space quantities corresponding to the 3D parameters in Eq. (1). We define the *effective opacity* at  $\mathbf{x}'$  as

$$\tilde{\alpha}_i(\mathbf{x}') = \alpha_i p_i(\mathbf{x}'). \quad (3)$$

and render the pixel feature by  $\alpha$ -blending:

$$\mathbf{F}(\mathbf{x}') = \sum_{i=1}^N \left( \prod_{j=1}^{i-1} (1 - \tilde{\alpha}_j(\mathbf{x}')) \right) \tilde{\alpha}_i(\mathbf{x}') \mathbf{f}_i. \quad (4)$$

**Limitations of GaussianFormer2.** To infer occupancy from Gaussians, GaussianFormer2 [11] introduces a *probabilistic Gaussian superposition* that treats each primitive  $\mathcal{G}_i$  as a local occupancy distribution and aggregates them multiplicatively. Concretely, the contribution of  $\mathcal{G}_i$  at a 3D location  $\mathbf{x}$  is

$$p_i(\mathbf{x}) = \exp\left(-\frac{1}{2}(\mathbf{x} - \boldsymbol{\mu}_i)^\top \boldsymbol{\Sigma}_i^{-1}(\mathbf{x} - \boldsymbol{\mu}_i)\right), \quad (5)$$

and, assuming independence across Gaussians, the aggregated occupancy becomes

$$p(\mathbf{x}) = 1 - \prod_{i=1}^N (1 - p_i(\mathbf{x})). \quad (6)$$

While efficient and conceptually simple, this formulation omits opacity  $\alpha_i$  in the geometry branch and relies solely on the spatial kernels. As a result, the occupancy inference is decoupled from the opacity used in image rendering, creating a mismatch between 2D rendering and 3D voxel aggregation.

**Why is this problematic?** In GaussianFormer2, geometry is aggregated without opacity (Eq. 6), but this does not cause issues because: 1) their semantic learning explicitly models opacity, and 2) it does not rely on 2D rendering during training, so no inconsistency arises. By contrast, our semantics are learned by *rendering* LE-Gaussian (Eq. 4) to images and aligning them to 2D open-vocabulary segmentations features, which is inherently opacity-aware. Using an opacity-agnostic voxel aggregation for geometry while supervising semantics via opacity-aware rendering introduces conflicting signals and unstable optimization.

**A Bernoulli approach.** A direct fix is to replace the spatial kernel  $p_i(\mathbf{x})$  with the *effective opacity*  $\tilde{\alpha}_i(\mathbf{x}) = \alpha_i p_i(\mathbf{x})$  and reuse the complementary-probability rule:

$$p(\mathbf{x}) = 1 - \prod_{i=1}^N (1 - \tilde{\alpha}_i(\mathbf{x})) = 1 - \prod_{i=1}^N (1 - \alpha_i p_i(\mathbf{x})), \quad (7)$$

which can be viewed as independent Bernoulli “hits” from overlapping Gaussians at  $\mathbf{x}$ . A similar opacity-based idea appears in Gaussian Opacity Fields [52] and in concurrent fully supervised closed-vocabulary method [1, 29].

However, we observe that the Bernoulli aggregation drives the learned opacities to *small* values, which enlarges

the gap between rendered features and per-Gaussian embeddings (see Sec. 3.4). This behavior likely arises because when multiple Gaussians overlap within a voxel, the Bernoulli union  $1 - \prod_i (1 - \alpha_i p_i)$  saturates rapidly toward 1; and for a fixed total mass  $\sum_i \alpha_i p_i$ , the union is maximized when each of the overlapping contributions are similar, making it difficult to learn differentiated opacities.

**A Poisson approach.** We adopt a Poisson formulation that treats each Gaussian’s local contribution as a nonnegative *event intensity* (mean count):

$$h_i(\mathbf{x}) \triangleq \alpha_i p_i(\mathbf{x}) \geq 0, \quad z(\mathbf{x}) = \sum_{i=1}^N h_i(\mathbf{x}), \quad (8)$$

where  $h_i$  is the expected contribution of Gaussian  $\mathcal{G}_i$  over a small voxel segment, and  $z(\mathbf{x})$  is the *mean measure* (cumulative expected count) from all Gaussians at  $\mathbf{x}$ . Modeling occupancy as the probability that a non-homogeneous Poisson process (NHPP) has produced at least one event at location  $\mathbf{x}$  gives a simple closed form. Let  $z(\mathbf{x})$  denote the accumulated mean measure at  $\mathbf{x}$ . A classical result for Poisson processes states that the probability of observing no event is  $\Pr[\text{no event at } \mathbf{x}] = \exp(-z(\mathbf{x}))$  [18, 32]. Interpreting “at least one event” as the space being occupied, the occupancy becomes a single exponential of the total mean measure:

$$p(\mathbf{x}) = 1 - \exp(-z(\mathbf{x})) = 1 - \exp\left(-\sum_{i=1}^N \alpha_i p_i(\mathbf{x})\right). \quad (9)$$

### 3.4. Progressive Temperature Decay

As shown in the semantic learning part of Fig. 2, we adopt Gaussian Splatting [17] to render LE-Gaussians into images. For semantic learning, we render LE-Gaussian features via Gaussian Splatting [17] to images. However, the  $\alpha$ -blending in Eq. (4) produces a *weighted sum* of per-ray contributions, so each pixel feature becomes a mixture of multiple Gaussian embeddings along the ray. Consequently, the supervision signal encourages the rendered mixture, rather than each individual Gaussian, to be language-aligned, creating a mismatch that later hampers G2O-based splatting. This ambiguity is further exacerbated in indoor scenes, where objects are numerous, fine-grained, and heavily overlapping in projection. Dr. Splat [16] mitigates this via hard *feature registration*: along a pixel ray it assigns the pixel’s CLIP embedding to only the Top- $k$  dominant Gaussians, yielding language-aligned vectors that are directly retrievable in 3D. While effective, this discrete selection causes sparse gradients, since supervision backpropagates only through the chosen Top- $k$  primitives.

Instead of a hard Top- $k$ , we reduce mixture ambiguity via a continuous and training-stable *opacity sharpening*. Let  $\alpha_i = \sigma(\alpha_i^{\text{logit}})$ , where  $\sigma$  is the sigmoid function and

$\alpha_i^{\text{logit}}$  is the model-predicted logit. We adopt a *tempered sigmoid*

$$\alpha_i = \sigma\left(\frac{\alpha_i^{\text{logit}}}{\tau}\right), \quad (10)$$

where smaller (near 0) temperature  $\tau$  values sharpen opacities towards  $\{0, 1\}$ , reducing feature mixing along the ray while maintaining gradient flow to all contributors (rather than a discrete subset). In practice, we employ a *progressive temperature decay* schedule during training, annealing  $\tau$  from  $T_{\max}$  to  $T_{\min}$  (default  $T_{\max}=1$ ,  $T_{\min}=10^{-3}$ ). Let  $r \in [0, 1]$  denote the normalized training progress, 0 means beginning, 1 means end. We use an *exponential* schedule

$$\tau(r) = \max\left\{T_{\min}, T_{\max} (T_{\min}/T_{\max})^r\right\},$$

which starts with smooth mixtures for stable optimization and gradually sharpens opacities for discriminative alignment. Compared with linear decay, our exponential schedule naturally allocates more iterations at low temperatures (see Fig. 3), empirically yielding *sharper* per-Gaussian opacities and stronger language alignment while preserving end-to-end differentiability throughout. With the proposed temperature-decay schedule, as  $\tau$  decreases, mixture blur is gradually reduced and supervision is increasingly transferred to individual Gaussians.

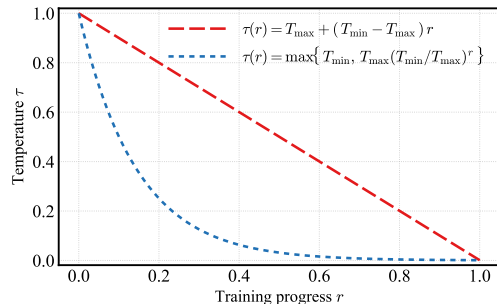


Figure 3. **Comparison of temperature schedules.** Linear decay decreases  $\tau$  uniformly, whereas our exponential schedule rapidly approaches  $T_{\min}$ , allocating more iterations for the model to adapt to the low-temperature regime.

### 3.5. Losses

We optimize the network with a composite objective that couples 3D geometry supervision with 2D language-aligned guidance as shown in Fig. 2. For occupancy, we follow [47] but use *binary* voxel supervision with focal loss  $L_{\text{focal}}$  and Lovász–Softmax  $L_{\text{lov}}$ , plus a scene-class affinity regularizer  $L_{\text{scal}}$  for spatial coherence. Geometry is further stabilized by a robust Huber depth loss  $L_{\text{depth}}$ . For semantics, we align image features from LE-Gaussians with frozen open-vocabulary segmentation features via a cosine objective  $L_{\text{feat}}$ . To exploit multi-view consistency without

Table 1. **Monocular results on Occ-ScanNet.** †We re-implement POP-3D [41] and LOcc [53] for the indoor monocular setting, and **supervise geometry with ground-truth binary occupancy** instead of the authors’ LiDAR-derived pseudo labels. For POP-3D, we project voxel centers to the image plane and sample language-aligned features at those locations to form a 3D grid of text-aligned embeddings for open-vocabulary reasoning. For LOcc, we prompt Qwen2.5-VL-7B [4] to extract object names and use Trident [35] to obtain training-free open-vocabulary segmentations, which yield stronger 2D masks on Occ-ScanNet. †Adopt DepthAnything-v2 [48] as the backbone and use the same input resolution and training recipe as ours for fair comparison.

Method	IoU	ceiling	floor	wall	window	chair	bed	sofa	table	tv	furniture	objects	mIoU
<i>Closed-vocabulary (full annotation)</i>													
TPVFormer [10]	33.39	6.96	32.97	14.41	9.10	24.01	41.49	45.44	28.61	10.66	35.37	25.31	24.94
GaussianFormer [13]	40.91	20.70	42.00	23.40	17.40	27.0	44.30	44.80	32.70	15.30	36.70	25.00	29.93
MonoScene [6]	41.60	15.17	44.71	22.41	12.55	26.11	27.03	35.91	28.32	6.57	32.16	19.84	24.62
ISO [50]	42.16	19.88	41.88	22.37	16.98	29.09	42.43	42.00	29.60	10.62	36.36	24.61	28.71
Surroundocc [45]	42.52	18.90	49.30	24.80	18.00	26.80	42.00	44.10	32.90	18.60	36.80	26.90	30.83
EmbodiedOcc [47]	53.55	39.60	50.40	41.40	31.70	40.90	55.00	61.40	44.00	36.10	53.90	42.20	45.15
EmbodiedOcc++ [42]	54.90	36.40	53.10	41.80	34.40	42.90	57.30	64.10	45.20	34.80	54.20	44.10	46.20
RoboOcc [57]	56.48	45.36	53.49	44.35	34.81	43.38	56.93	63.35	46.35	36.12	55.48	44.78	47.76
<i>Open-vocabulary (geometry-only annotation)</i>													
POP-3D† [41]	35.32	0.00	23.89	16.59	0.01	4.62	8.65	2.01	7.61	0.00	2.14	0.08	5.96
LOcc† [53]	36.70	0.00	24.40	17.37	1.83	9.31	10.73	23.42	11.29	0.01	3.15	0.19	9.25
LegoOcc (Ours)	59.50	17.81	41.65	28.52	18.91	19.32	33.05	34.92	19.16	5.36	5.88	6.94	21.05

2D labels, we re-render nearby views (default: 5 frames) and apply the same feature alignment. The final objective is

$$L_{\text{total}} = \lambda_{\text{focal}} L_{\text{focal}} + \lambda_{\text{lov}} L_{\text{lov}} + \lambda_{\text{scal}} L_{\text{scal}} + \lambda_{\text{feat}} L_{\text{feat}} + \lambda_{\text{depth}} L_{\text{depth}}. \quad (11)$$

## 4. Experiments

### 4.1. Datasets and Metrics

**Dataset.** We train and evaluate on Occ-ScanNet [50], where each sample provides a  $60 \times 60 \times 36$  voxel grid covering a  $4.8\text{m} \times 4.8\text{m} \times 2.88\text{m}$  volume. The dataset comprises 12 classes in total—11 semantic categories (*ceiling, floor, wall, window, chair, bed, sofa, table, television, furniture, objects*) plus *empty*, and is split into 45,755 training and 19,764 validation samples.

**Task setup.** We study the *monocular* setting, where a single RGB image serves as input. All experiments on Occ-ScanNet are conducted *without* semantic voxel annotations during training: geometry is supervised by binary occupancy labels, while semantics are learned via language-aligned feature rendering (Sec. 3.4). Evaluation uses the semantic labels for quantitative assessment.

**Metrics.** Following prior work [47, 50], evaluation is restricted to the current camera frustum. We report: 1) overall occupancy IoU and 2) per-class IoU over the 11 semantic categories, together with the mean IoU (mIoU).

### 4.2. Implementation Details

We adopt Depth-Anything V2 [48] as our depth backbone, which has been used as a geometry prior in [47, 50]. Building on this, we construct Gaussian primitives using a surface-point expansion strategy similar to [2]. All models are trained for 10 epochs with a batch size of 4, optimizing with AdamW [26]; the learning rate is initialized at  $2 \times 10^{-4}$  and follows a cosine decay schedule [25] with linear warmup, with weight decay set to 0.01. We apply gradient clipping [27] with a maximum norm of 1.0, and resize each image so that its longer side is 518 pixels while preserving aspect ratio. We train all our model using 4 NVIDIA GeForce RTX 4090 GPUs.

### 4.3. Main Results

To assess the effectiveness of our approach, we conduct a comprehensive evaluation on the Occ-ScanNet benchmark [50] and present both overall and per-class Intersection-over-Union (IoU) as well as mean IoU (mIoU) in Tab. 1. For clarity, rows marked blue denotes *closed-vocabulary* (full annotation) settings, while rows in orange denote *open-vocabulary* (geometry-only annotation); darker shades highlight our method.

From Tab. 1, we observe that using geometry-only annotation the re-implemented baselines POP-3D [41] and

LOcc [53] perform poorly, obtains only 35.32/5.96 and 36.70/9.25 IoU/mIoU, respectively. In contrast, our model reaches 59.50 IoU and 21.05 mIoU, outperforming both by a large margin. Notably, LegoOcc achieves the highest IoU among all entries, indicating that the proposed design effectively recovers occupancy without semantic voxel labels. The remaining performance gap between full-annotation methods and geometry-only ones in mIoU highlights the intrinsic difficulty of category calibration for open-vocabulary occupancy, particularly under class ambiguity. We further illustrate these problem in our appendix.

#### 4.4. Ablation Studies

We use the same coloring convention as in the main results for [closed-vocabulary](#) and [open-vocabulary](#) settings. When a table reports *only* the open-vocabulary setting results, background coloring is omit for brevity. More ablations and analyses are provided in our appendix.

Table 2. **Ablation on the Gaussian-to-Occupancy operator.** We compare three aggregation rules: GaussianFormer2, Bernoulli, and Poisson, under both *closed-* and *open-* vocabulary settings.

Operation	mIoU	IoU
GaussianFormer2	51.88	56.96
Bernoulli	51.68	58.06
Poisson	52.80	59.24
GaussianFormer2	0.00	0.00
Bernoulli	17.25	46.65
Poisson	21.05	59.50

**Ablation on Gaussian-to-Occupancy (G2O).** As shown in Tab. 2, replacing the operator from GaussianFormer2 [11] with our Poisson-based G2O consistently improves performance under the *closed-vocabulary* setting, 56.96→59.24 IoU and 51.88→52.80 mIoU. The advantage is even more pronounced in the *open-vocabulary* case, where our Poisson G2O achieves 59.50 IoU and 21.05 mIoU, surpassing the Bernoulli variant by +12.85 IoU and +3.80 mIoU. These results indicate that explicitly incorporating opacity via a Poisson-based compositing framework yields more faithful voxel aggregation.

Table 3. **Ablation on temperature scheduling.** We vary the temperature range ( $T_{min}, T_{max}$ ), the test-time temperature  $\tau_{test}$ , and the scheduling strategy. “×” denotes no schedule.

$T_{min}$	$T_{max}$	$\tau_{test}$	scheduler	mIoU	IoU
1.0	1.0	1	×	18.15	59.19
1.0	1.0	1e-3	×	12.83	32.52
1e-3	1e-3	1e-3	×	0.00	0.00
1e-3	1.0	1e-3	linear	2.30	7.60
1e-2	1.0	1e-2	exp	20.85	59.25
1e-3	1.0	1e-3	exp	21.05	59.50
1e-4	1.0	1e-4	exp	20.37	58.54

**Ablation on temperature scheduling.** As reported in Tab. 3, fixing  $\tau=1$  throughout training and testing (*i.e.*, no schedule) yields reasonable geometry (59.19 IoU) but poor semantics (18.15 mIoU), indicating substantial per-ray feature mixing degrades semantic discrimination. Using mismatched temperatures ( $\tau_{train}=1, \tau_{test}=10^{-3}$ ) severely degrades geometry (32.52 IoU) due to a train–test distribution shift. Keeping a constant low temperature ( $\tau=10^{-3}$ ) collapses optimization entirely, underscoring the necessity of progressive decay. A linear decay from  $1 \rightarrow 10^{-3}$  with few iterations near  $\tau \approx 0$  also underperforms (2.30 mIoU/7.60 IoU), suggesting that allocating too few steps in the low-temperature regime inadequately sharpen per-Gaussian opacities. In contrast, our exponential schedule, which allocates more iterations to the low-temperature regime, achieves the best results: 21.05 mIoU/59.50 IoU with  $(T_{min}, T_{max})=(10^{-3}, 1)$  and  $\tau_{test}=10^{-3}$ . Lowering  $T_{min}$  to  $10^{-4}$  slightly hurts performance (20.37 mIoU/58.54 IoU), suggesting over-sharpening amplifies noise. These results demonstrate that progressive temperature decay effectively reduces feature mixing and yields sharper, more discriminative Gaussian embeddings.

Table 4. **Model profile.** FPS is measured on the same machine with a single RTX 4090 GPU, averaged over 1,000 runs after 100 warm-up runs.

Model	mIoU	IoU	FPS
ISO [50]	28.71	42.16	3.81
EmbodiedOcc [47]	45.15	53.55	11.48
POP-3D [41]	5.96	35.32	10.21
LOcc [53]	9.25	36.70	8.93
Ours	21.05	59.50	22.47

**Model profile.** We summarize the model profile in Tab. 4. Note that ISO [50] and EmbodiedOcc [47] rely on closed-set classification heads, while open-vocabulary methods compare occupancy features with language embeddings [30] via cosine similarity.

#### 4.5. Qualitative Visualization

We present qualitative results under both closed and open vocabulary settings. As shown in Fig. 4, our open-vocabulary model is evaluated against the closed-set semantics of Occ-ScanNet [50]. Across diverse scenes, the predicted occupancy aligns closely with ground-truth labels, indicating strong geometric accuracy and semantic generalization to the dataset taxonomy. Beyond this closed set, Fig. 5 presents open-vocabulary predictions obtained by querying arbitrary given categories. For each image, a VLM [4] extracts object *nouns* as text queries, which our model uses to produce the corresponding 3D semantic occupancies. More qualitative visualizations are provided in our appendix, including text-conditioned 3D grounding ex-

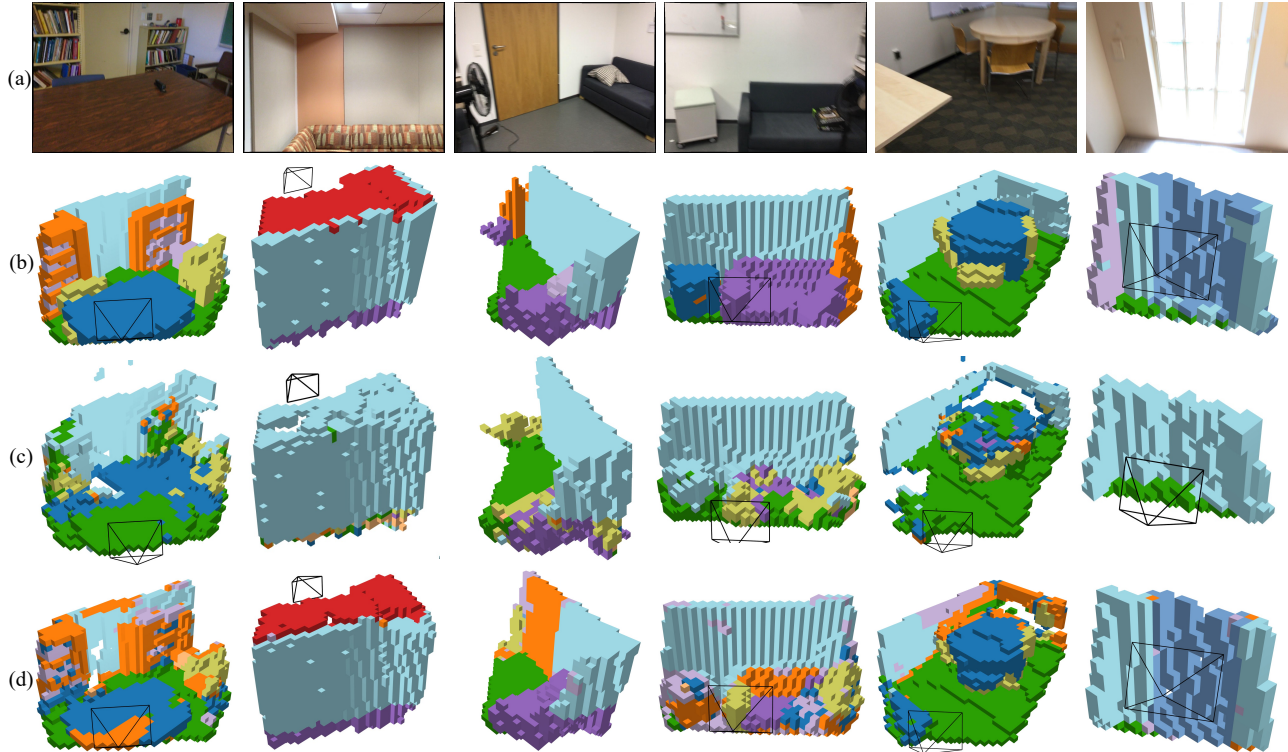


Figure 4. **Qualitative results on Occ-ScanNet.** From top to bottom: (a) input images; (b) ground-truth semantic occupancy; (c) results from our re-implemented LOcc [53]; (d) our method. Both (c) and (d) are trained with geometry-only annotations and evaluated on the closed-vocabulary annotation of Occ-ScanNet.

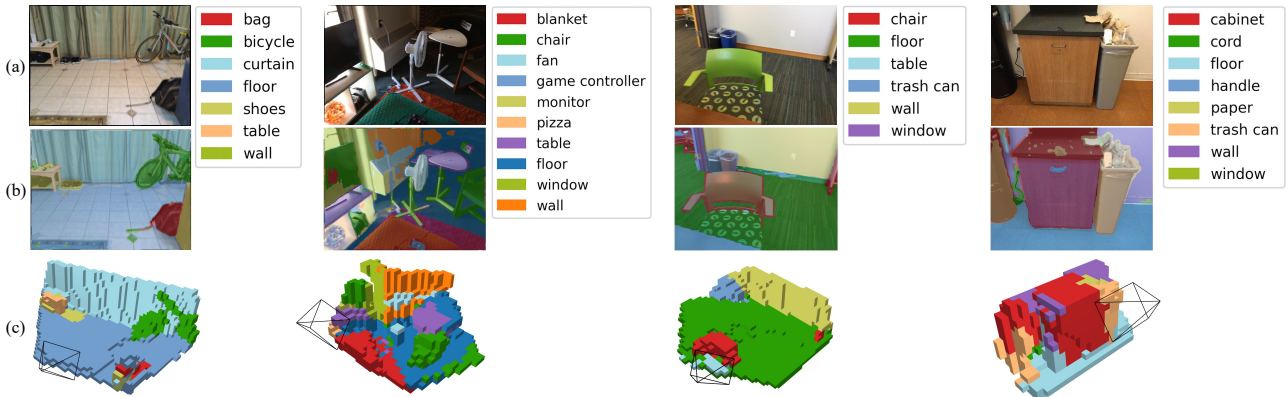


Figure 5. **Open-vocabulary qualitative results.** Legends list the *VLM-extracted object nouns* used as text queries. (a) Input image. (b) Open-vocabulary 2D segmentation for queried nouns. (c) Our 3D open-vocabulary occupancy colored by the same categories.

amples. These results demonstrate the model’s ability to localize and identify free-form indoor categories in 3D.

## 5. Conclusion

We introduced a monocular open-vocabulary occupancy framework for large-scale indoor scenes, where category distributions are long-tailed and open-ended. Central to our

approach is a reformulated, opacity-aware Poisson-based Gaussian-to-Occupancy operator that enables Gaussians to serve as a unified semantic–geometric intermediate representation. Complementing this, we propose a Progressive Temperature Decay schedule to mitigate feature dilution during splatting and enhance discriminability. Extensive experiments on Occ-ScanNet demonstrate strong performance. Our method supports text-conditioned queries and

scales across embodied tasks without closed-vocabulary constraints, paving the way for wider occupancy use in real-world embodied applications.

## References

- [1] Anonymous. S2GO: Streaming sparse gaussian occupancy. In *Submitted to The Fourteenth International Conference on Learning Representations*, 2025. under review. 4
- [2] Anonymous. VGMOcc: Sparse gaussian occupancy prediction with visual geometry model priors. In *Submitted to The Fourteenth International Conference on Learning Representations*, 2025. under review. 6
- [3] Armen Avetisyan, Manuel Dahnert, Angela Dai, Manolis Savva, Angel X. Chang, and Matthias Niessner. Scan2cad: Learning cad model alignment in rgb-d scans. In *The IEEE Conference on Computer Vision and Pattern Recognition (CVPR)*, 2019. 2
- [4] Shuai Bai, Keqin Chen, Xuejing Liu, Jialin Wang, Wenbin Ge, Sibao Song, Kai Dang, Peng Wang, Shijie Wang, Jun Tang, Humen Zhong, Yuanzhi Zhu, Mingkun Yang, Zhao-hai Li, Jianqiang Wan, Pengfei Wang, Wei Ding, Zheren Fu, Yiheng Xu, Jiabo Ye, Xi Zhang, Tianbao Xie, Zesen Cheng, Hang Zhang, Zhibo Yang, Haiyang Xu, and Junyang Lin. Qwen2.5-vl technical report. *arXiv preprint arXiv:2502.13923*, 2025. 6, 7
- [5] Simon Boeder, Fabian Gigengack, and Benjamin Risse. Langocc: Self-supervised open vocabulary occupancy estimation via volume rendering. *arXiv preprint arXiv:2407.17310*, 2024. 2, 3
- [6] Anh-Quan Cao and Raoul De Charette. Monoscene: Monocular 3d semantic scene completion. In *Proceedings of the IEEE/CVF Conference on Computer Vision and Pattern Recognition*, pages 3991–4001, 2022. 2, 3, 6
- [7] Loick Chambon, Eloi Zablocki, Alexandre Boulch, Mickael Chen, and Matthieu Cord. Gaussrender: Learning 3d occupancy with gaussian rendering. In *Proceedings of the IEEE/CVF International Conference on Computer Vision*, pages 27010–27020, 2025. 1
- [8] Zichao Dong, Hang Ji, Weikun Zhang, Xufeng Huang, and Junbo Chen. Og: Equip vision occupancy with instance segmentation and visual grounding. *arXiv preprint arXiv:2307.05873*, 2023. 3
- [9] Yuhang Gao, Xiang Xiang, Sheng Zhong, and Guoyou Wang. Loc: A general language-guided framework for open-set 3d occupancy prediction. *arXiv preprint arXiv:2510.22141*, 2025. 3
- [10] Yuanhui Huang, Wenzhao Zheng, Yunpeng Zhang, Jie Zhou, and Jiwen Lu. Tri-perspective view for vision-based 3d semantic occupancy prediction. In *Proceedings of the IEEE/CVF conference on computer vision and pattern recognition*, pages 9223–9232, 2023. 6
- [11] Yuanhui Huang, Amonnut Thammatadrakoon, Wenzhao Zheng, Yunpeng Zhang, Dalong Du, and Jiwen Lu. Gaussianformer-2: Probabilistic gaussian superposition for efficient 3d occupancy prediction. *arXiv preprint arXiv:2412.04384*, 2024. 1, 2, 4, 7
- [12] Yuanhui Huang, Wenzhao Zheng, Borui Zhang, Jie Zhou, and Jiwen Lu. Selfocc: Self-supervised vision-based 3d occupancy prediction. In *Proceedings of the IEEE/CVF Conference on Computer Vision and Pattern Recognition (CVPR)*, pages 19946–19956, 2024. 3
- [13] Yuanhui Huang, Wenzhao Zheng, Yunpeng Zhang, Jie Zhou, and Jiwen Lu. Gaussianformer: Scene as gaussians for vision-based 3d semantic occupancy prediction. In *European Conference on Computer Vision*, pages 376–393. Springer, 2024. 1, 2, 3, 6
- [14] Haochen Jiang, Yueming Xu, Yihan Zeng, Hang Xu, Wei Zhang, Jianfeng Feng, and Li Zhang. Openocc: Open vocabulary 3d scene reconstruction via occupancy representation. In *IEEE/RSJ International Conference on Intelligent Robots and Systems (IROS)*, 2024. 3
- [15] KJ Joseph, Salman Khan, Fahad Shahbaz Khan, and Vineeth N Balasubramanian. Towards open world object detection. In *Proceedings of the IEEE/CVF conference on computer vision and pattern recognition*, pages 5830–5840, 2021. 1
- [16] Kim Jun-Seong, Kim GeonU, Kim Yu-Ji, Yu-Chiang Frank Wang, Jaesung Choe, and Tae-Hyun Oh. Dr. splat: Directly referring 3d gaussian splatting via direct language embedding registration. In *CVPR*, 2025. 5
- [17] Bernhard Kerbl, Georgios Kopanas, Thomas Leimkühler, and George Drettakis. 3d gaussian splatting for real-time radiance field rendering. *ACM Trans. Graph.*, 42(4):139–1, 2023. 2, 3, 5
- [18] J. F. C. Kingman. *Poisson processes*. The Clarendon Press Oxford University Press, New York, 1993. Oxford Science Publications. 5
- [19] Peizheng Li, Shuxiao Ding, You Zhou, Qingwen Zhang, Onat Inak, Larissa Triess, Niklas Hanselmann, Marius Cordts, and Andreas Zell. Ago: Adaptive grounding for open world 3d occupancy prediction. *arXiv preprint arXiv:2504.10117*, 2025. 2, 3
- [20] Yiming Li, Zhiding Yu, Christopher Choy, Chaowei Xiao, Jose M Alvarez, Sanja Fidler, Chen Feng, and Anima Anandkumar. Voxformer: Sparse voxel transformer for camera-based 3d semantic scene completion. In *Proceedings of the IEEE/CVF conference on computer vision and pattern recognition*, pages 9087–9098, 2023. 1
- [21] Zhiqi Li, Zhiding Yu, David Austin, Mingsheng Fang, Shiyi Lan, Jan Kautz, and Jose M Alvarez. FB-OCC: 3D occupancy prediction based on forward-backward view transformation. *arXiv:2307.01492*, 2023. 3
- [22] Rui Liu, Wenguan Wang, and Yi Yang. Volumetric environment representation for vision-language navigation. In *Proceedings of the IEEE/CVF conference on computer vision and pattern recognition*, pages 16317–16328, 2024. 1
- [23] Ruixun Liu, Lingyu Kong, Derun Li, and Hang Zhao. Oc-cvla: Vision-language-action model with implicit 3d occupancy supervision. *arXiv preprint arXiv:2509.05578*, 2025. 1
- [24] Shilong Liu, Zhaoyang Zeng, Tianhe Ren, Feng Li, Hao Zhang, Jie Yang, Qing Jiang, Chunyuan Li, Jianwei Yang, Hang Su, et al. Grounding dino: Marrying dino with

- grounded pre-training for open-set object detection. In *European conference on computer vision*, pages 38–55. Springer, 2024. 3
- [25] Ilya Loshchilov and Frank Hutter. Sgdr: Stochastic gradient descent with warm restarts. *arXiv preprint arXiv:1608.03983*, 2016. 6
- [26] Ilya Loshchilov and Frank Hutter. Decoupled weight decay regularization. *arXiv preprint arXiv:1711.05101*, 2017. 6
- [27] Razvan Pascanu, Tomas Mikolov, and Yoshua Bengio. On the difficulty of training recurrent neural networks. In *International conference on machine learning*, pages 1310–1318. Pmlr, 2013. 6
- [28] Jonah Philion and Sanja Fidler. Lift, splat, shoot: Encoding images from arbitrary camera rigs by implicitly unprojecting to 3d. In *European conference on computer vision*, pages 194–210. Springer, 2020. 3
- [29] Rui Qian, Haozhi Cao, Tianchen Deng, Shenghai Yuan, and Lihua Xie. Splatssc: Decoupled depth-guided gaussian splatting for semantic scene completion, 2025. 4
- [30] Alec Radford, Jong Wook Kim, Chris Hallacy, Aditya Ramesh, Gabriel Goh, Sandhini Agarwal, Girish Sastry, Amanda Askell, Pamela Mishkin, Jack Clark, et al. Learning transferable visual models from natural language supervision. In *International conference on machine learning*, pages 8748–8763. Pmlr, 2021. 2, 7
- [31] Tianhe Ren, Shilong Liu, Ailing Zeng, Jing Lin, Kunchang Li, He Cao, Jiayu Chen, Xinyu Huang, Yukang Chen, Feng Yan, et al. Grounded sam: Assembling open-world models for diverse visual tasks. *arXiv preprint arXiv:2401.14159*, 2024. 3
- [32] S.M. Ross. *Stochastic processes*. Wiley, 1996. 5
- [33] Jin-Chuan Shi, Miao Wang, Hao-Bin Duan, and Shao-Hua Guan. Language embedded 3d gaussians for open-vocabulary scene understanding. *arXiv preprint arXiv:2311.18482*, 2023. 2
- [34] Yiang Shi, Tianheng Cheng, Qian Zhang, Wenyu Liu, and Xinggang Wang. Occupancy as set of points. In *European Conference on Computer Vision*, pages 72–87. Springer, 2024. 2
- [35] Yuheng Shi, Minjing Dong, and Chang Xu. Harnessing vision foundation models for high-performance, training-free open vocabulary segmentation. *arXiv preprint arXiv:2411.09219*, 2024. 2, 6
- [36] Zhan Shi, Song Wang, Junbo Chen, and Jianke Zhu. A coarse-to-fine approach to multi-modality 3d occupancy grounding. *arXiv preprint arXiv:2508.01197*, 2025. 2
- [37] Shuran Song, Fisher Yu, Andy Zeng, Angel X Chang, Manolis Savva, and Thomas Funkhouser. Semantic scene completion from a single depth image. In *Proceedings of the IEEE conference on computer vision and pattern recognition*, pages 1746–1754, 2017. 2
- [38] Zhiyu Tan, Zichao Dong, Cheng Zhang, Weikun Zhang, Hang Ji, and Hao Li. Ovo: Open-vocabulary occupancy, 2023. 2, 3
- [39] Pin Tang, Zhongdao Wang, Guoqing Wang, Jilai Zheng, Xianguan Ren, Bailan Feng, and Chao Ma. Sparseocc: Rethinking sparse latent representation for vision-based semantic occupancy prediction. In *Proceedings of the IEEE/CVF Conference on Computer Vision and Pattern Recognition*, pages 15035–15044, 2024. 1
- [40] Emanuele Vespa, Nikolay Nikolov, Marius Grimm, Luigi Nardi, Paul H. J. Kelly, and Stefan Leutenegger. Efficient octree-based volumetric slam supporting signed-distance and occupancy mapping. *IEEE Robotics and Automation Letters*, 3(2):1144–1151, 2018. 2
- [41] Antonin Vobecky, Oriane Siméoni, David Hurych, Spyridon Gidaris, Andrei Bursuc, Patrick Pérez, and Josef Sivic. Pop-3d: Open-vocabulary 3d occupancy prediction from images. *Advances in Neural Information Processing Systems*, 36:50545–50557, 2023. 3, 6, 7
- [42] Hao Wang, Xiaobao Wei, Xiaoan Zhang, Jianing Li, Chengyu Bai, Ying Li, Ming Lu, Wenzhao Zheng, and Shanghang Zhang. Embodiedocc++: Boosting embodied 3d occupancy prediction with plane regularization and uncertainty sampler. *arXiv preprint arXiv:2504.09540*, 2025. 1, 3, 6
- [43] Yida Wang, David Joseph Tan, Nassir Navab, and Federico Tombari. Forknet: Multi-branch volumetric semantic completion from a single depth image, 2019. 2
- [44] Julong Wei, Shanshuai Yuan, Pengfei Li, Qingda Hu, Zhongxue Gan, and Wenchao Ding. Occllama: An occupancy-language-action generative world model for autonomous driving. *arXiv preprint arXiv:2409.03272*, 2024. 1
- [45] Yi Wei, Linqing Zhao, Wenzhao Zheng, Zheng Zhu, Jie Zhou, and Jiwen Lu. Surroundocc: Multi-camera 3d occupancy prediction for autonomous driving. In *Proceedings of the IEEE/CVF International Conference on Computer Vision*, pages 21729–21740, 2023. 1, 6
- [46] Shun-Cheng Wu, Kesuke Tateno, Nassir Navab, and Federico Tombari. Scfusion: Real-time incremental scene reconstruction with semantic completion. In *2020 International Conference on 3D Vision (3DV)*, pages 801–810, 2020. 2
- [47] Yuqi Wu, Wenzhao Zheng, Sicheng Zuo, Yuanhui Huang, Jie Zhou, and Jiwen Lu. Embodiedocc: Embodied 3d occupancy prediction for vision-based online scene understanding. *arXiv preprint arXiv:2412.04380*, 2024. 1, 2, 3, 5, 6, 7
- [48] Lihe Yang, Bingyi Kang, Zilong Huang, Zhen Zhao, Xiaogang Xu, Jiashi Feng, and Hengshuang Zhao. Depth anything v2. *Advances in Neural Information Processing Systems*, 37:21875–21911, 2024. 6
- [49] Jiawei Yao, Chuming Li, Keqiang Sun, Yingjie Cai, Hao Li, Wanli Ouyang, and Hongsheng Li. Ndc-scene: Boost monocular 3d semantic scene completion in normalized device coordinates space. In *2023 IEEE/CVF International Conference on Computer Vision (ICCV)*, pages 9421–9431. IEEE Computer Society, 2023. 2, 3
- [50] Hongxiao Yu, Yuqi Wang, Yuntao Chen, and Zhaoxiang Zhang. Monocular occupancy prediction for scalable indoor scenes. In *European Conference on Computer Vision*, pages 38–54. Springer, 2024. 1, 2, 3, 6, 7
- [51] Qiucheng Yu, Yuan Xie, and Xin Tan. Shtocc: Effective 3d occupancy prediction with sparse head and tail voxels. *arXiv preprint arXiv:2505.22461*, 2025. 1

- [52] Zehao Yu, Torsten Sattler, and Andreas Geiger. Gaussian opacity fields: Efficient adaptive surface reconstruction in unbounded scenes. *ACM Transactions on Graphics*, 2024. [4](#)
- [53] Zhu Yu, Bowen Pang, Lizhe Liu, Runmin Zhang, Qiang Li, Si-Yuan Cao, Maochun Luo, Mingxia Chen, Sheng Yang, and Hui-Liang Shen. Language driven occupancy prediction. In *Proceedings of the IEEE/CVF International Conference on Computer Vision*, pages 7548–7558, 2025. [2](#), [3](#), [6](#), [7](#), [8](#)
- [54] Chubin Zhang, Juncheng Yan, Yi Wei, Jiabin Li, Li Liu, Yansong Tang, Yueqi Duan, and Jiwen Lu. Occnerf: Self-supervised multi-camera occupancy prediction with neural radiance fields. *CoRR*, abs/2312.09243, 2023. [3](#)
- [55] Yifan Zhang, Bingyi Kang, Bryan Hooi, Shuicheng Yan, and Jiashi Feng. Deep long-tailed learning: A survey. *IEEE transactions on pattern analysis and machine intelligence*, 45(9):10795–10816, 2023. [1](#)
- [56] Yunpeng Zhang, Zheng Zhu, and Dalong Du. Occformer: Dual-path transformer for vision-based 3d semantic occupancy prediction. In *Proceedings of the IEEE/CVF International Conference on Computer Vision (ICCV)*, pages 9433–9443, 2023. [1](#)
- [57] Zhang Zhang, Qiang Zhang, Wei Cui, Shuai Shi, Yijie Guo, Gang Han, Wen Zhao, Hengle Ren, Renjing Xu, and Jian Tang. Roboocc: Enhancing the geometric and semantic scene understanding for robots. *arXiv preprint arXiv:2504.14604*, 2025. [3](#), [6](#)
- [58] Jilai Zheng, Pin Tang, Zhongdao Wang, Guoqing Wang, Xi-angxuan Ren, Bailan Feng, and Chao Ma. Veon: Vocabulary-enhanced occupancy prediction. In *European Conference on Computer Vision*, pages 92–108. Springer, 2024. [2](#), [3](#)
- [59] Shijie Zhou, Haoran Chang, Sicheng Jiang, Zhiwen Fan, Zehao Zhu, Dejie Xu, Pradyumna Chari, Suyu You, Zhangyang Wang, and Achuta Kadambi. Feature 3dgs: Supercharging 3d gaussian splatting to enable distilled feature fields. In *Proceedings of the IEEE/CVF Conference on Computer Vision and Pattern Recognition*, pages 21676–21685, 2024. [2](#)